JACS
JOURNAL OF THE AMERICAN CHEMICAL SOCIETY

Communication

pubs.acs.org/JACS

X-ray Crystal Structure of Phosphodiesterase 2 in Complex with a Highly Selective, Nanomolar Inhibitor Reveals a Binding-Induced Pocket Important for Selectivity

Jian Zhu,[‡,†] Qiqi Yang,[‡] Dandan Dai,[‡] and Qiang Huang*[,‡]

[‡]State Key Laboratory of Genetic Engineering, School of Life Sciences, Fudan University, Shanghai 200433, China
[†]Shanghai Medicilon Inc., Shanghai 201299, China

Supporting Information

ABSTRACT: To better understand the structural origins of inhibitor selectivity of human phosphodieasterase families (PDEs 1−11), here we report the X-ray crystal structure of PDE2 in complex with a highly selective, nanomolar inhibitor (BAY60-7550) at 1.9 Å resolution, and the structure of apo PDE2 at 2.0 Å resolution. The crystal structures reveal that the inhibitor binds to the PDE2 active site by using not only the conserved glutamine-switch mechanism for substrate binding, but also a binding-induced, hydrophobic pocket that was not reported previously. *In silico* affinity profiling by molecular docking indicates that the inhibitor binding to this pocket contributes significantly to the binding affinity and thereby improves the inhibitor selectivity for PDE2. Our results highlight a structure-based design strategy that exploits the potential binding-induced pockets to achieve higher selectivity in the PDE inhibitor development.

Human cyclic nucleotide phosphodiesterase families (namely PDEs 1−11) play a critical role in regulating cell signal cascades by hydrolyzing the intracellular second messengers, cAMP and cGMP. Due to their unique tissue distributions and cellular functions, PDEs are involved in a wide variety of disease states.[1,2] To date, several drugs targeting at PDE3,[3] PDE4,[4] and PDE5[5] have been approved for clinical use. Therefore, it is widely believed that developing selective inhibitors for specific PDE isoforms and thereby reducing potential adverse effects in therapeutic use are possible.

Phosphodiesterase 2 (PDE2) is a dual-substrate specific PDE to hydrolyze both cAMP and cGMP, which have attracted much attention as a valuable therapeutic target for central nervous system (CNS) disorders,[6] including Alzheimer's disease.[7] BAY60-7550 (**1** in Figure 1A) is an important, nanomolar inhibitor of PDE2. Recently, preclinical studies performed in behavioral models have confirmed its efficacy in enhancing learning, memory, and cognitive function.[7−12] BAY60-7550 has been shown to be 50-fold more selective for PDE2 compared to PDE1, and more than 100-fold selective compared to PDE3B, PDE4B, PDE5, PDE7B, PDE8A, PDE10A, and PDE11A.[8] Because the active sites of various PDEs are very similar, to avoid the promiscuous problem of inhibitors, it is very interesting to understand: Why does **1** possess such high selectivity for PDE2? What are the structural origins of the high selectivity? To answer these questions, structural studies of PDEs[13] suggested that a complex structure of PDE2 with the selective inhibitor would be very enlightening. However, except for a complex with a nonspecific, micromolar inhibitor, IBMX,[14] so far in the Protein Data Bank

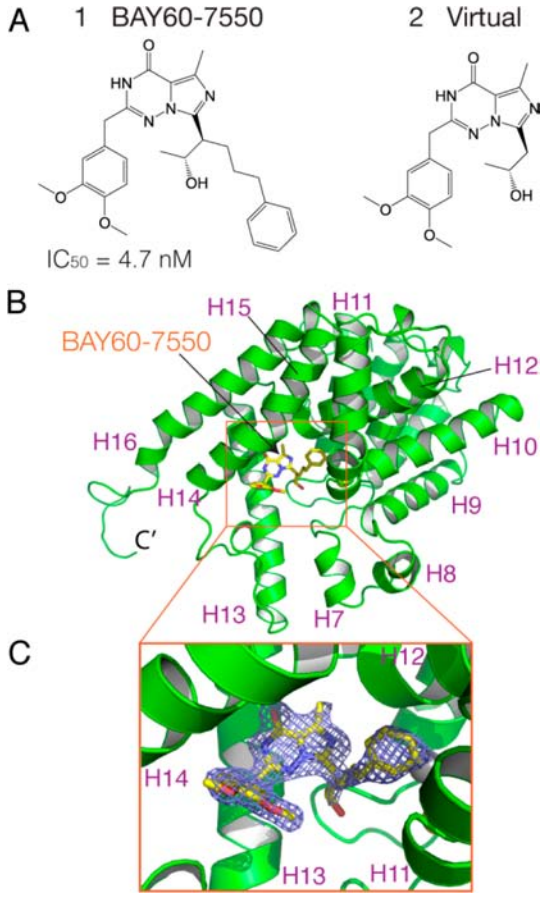

Figure 1. Crystal structure of PDE2A in complex with BAY60-7550. (A) Chemical structures of BAY60-7550 and a virtual molecule without the propylphenyl group. (B) The overall structure (for clarity, helices H1−H6 are not labeled). (C) Omit $F_o - F_c$ electron density map at a contour level of 3.0σ.

Received: May 11, 2013
Published: July 30, 2013

(PDB) there is only one PDE2 structure in complex with a nanomolar inhibitor (IC_{50} = 45 nM),[15] which was only recently made available. The structural origins of the high selectivity of **1** remain unclear. To address this issue and to provide structural insights into the inhibitor selectivity, here we report the crystal structure of the PDE2A catalytic domain (a.a. 578−919) in complex with **1**, and the corresponding apo structure for comparison.

The PDE2A catalytic domain for X-ray crystallography study was expressed in *E. coli* cells with a Trx tag[16] fused to the N-terminus, which significantly improved the protein solubility as compared to other fusion partners, e.g., SUMO and GST. The protein was purified in a monomeric form via a few chromatography steps (see details in Supporting Information [SI] and Figure S1, in particular). Finally, we crystallized and determined the complex structure of PDA2A with **1** at a resolution of 1.9 Å and the apo structure at a resolution of 2.0 Å (Table S1 in SI). The solved structures indicate that the apo and complex crystals belong to the same triclinic space group *P*1, and there are four identical protein molecules in one asymmetric unit cell. These two structures could be superimposed very well with a C_α-RMSD (root-mean-square deviation) of ∼0.26 Å (Figure S2A in SI). As shown in Figure 1B, the PDE2A catalytic domain consists of 16 helices that are compactly arranged; the active site pocket is located in the junction region of the helices H11−H14 and enclosed by highly conserved residues in PDEs. Two metal ions, Mg^{2+} and Zn^{2+}, are embedded in the bottom of the active site by coordination with histidines, aspartic acids, and water molecules (Figures 2A and S3B [SI]).

The electron density maps clearly show that **1** directly binds to the active site of PDE2A (Figures 1C and S3B [SI]), providing the first crystal structure of PDE2 in complex with a highly selective inhibitor with an IC_{50} < 10 nM. Previous studies have shown that in the apo structure the H7−H8 segment (i.e., H-loop) of the catalytic domain (Figure 1B) may adopt either a 'closed' state or an 'open' conformation for ligand binding to the active site.[14] Here, our apo structure shows that this segment swings out from the active site and is in an open-like conformation, implying that the crystal packing did not prevent the inhibitor from binding to the active site. Indeed, the binding mode of **1** in each PDE2A in the asymmetric unit cell is almost the same (Figure S2B in SI).

Very interestingly, the binding mode of **1** in the PDE2A active site reveals an induced hydrophobic subpocket for the inhibitor binding. Structural study of PDE4 has shown that a ligand may bind to three subpockets in the active site: the pocket containing the glutamine-switch and hydrophobic clamp (Q-pocket), the metal binding pocket (M-pocket), and the solvent-filled side pocket (S-pocket).[17] The corresponding subpockets and related residues in PDE2A have been shown in the crystal structure in Figure 2A. As seen for these three known subpockets, **1** mainly occupies the Q-pocket, contacts the M-pocket only with a few atoms, but does not interact with the S-pocket. Besides these subpockets, we found that the hydrophobic propylphenyl group of **1** binds to a new subpocket between helices H11 and H14, which is formed mainly by hydrophobic residues: Leu770, Leu809, Ile866, Ile870, His773, and Leu774 (in yellow in Figure 2A). Therefore, we designated it as H-pocket (i.e., hydrophobic pocket). As compared with the apo structure, it is very clear that, upon the inhibitor binding, the residues that enclose the H-pocket undergo significant conformational changes to accommodate the

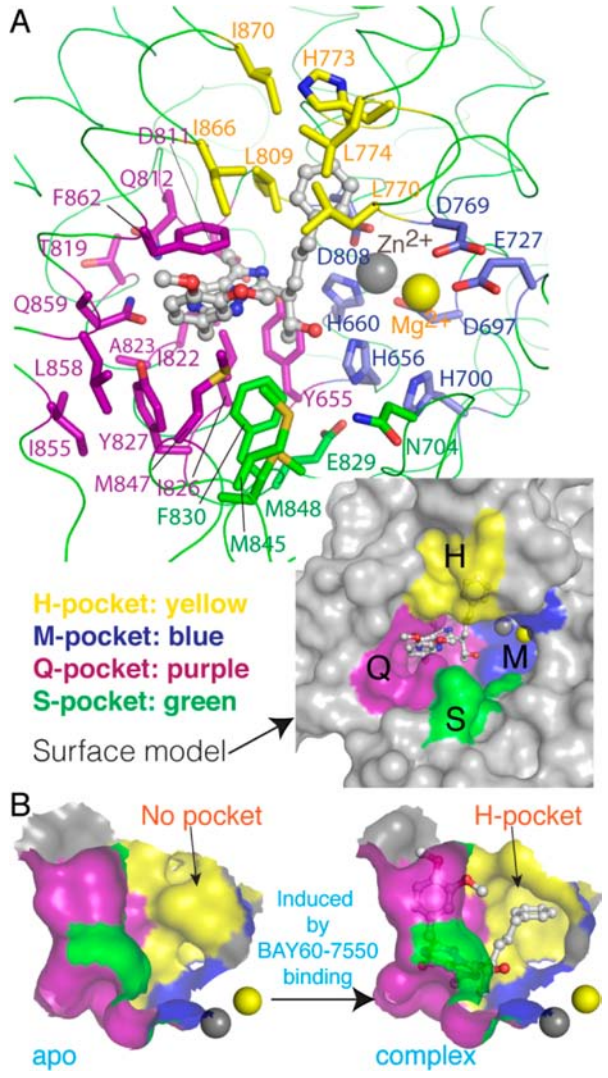

Figure 2. Binding mode of BAY60-7550 in PDE2A. (A) Surrounding residues of four binding subpockets shown by stick models and surface models, respectively. (B) H-pocket induced by the inhibitor binding.

propylphenyl group (Figure 2B), for example, the binding leads the side chain of Leu770 to a shift of about 3.2 Å, which was calculated according to the coordinates of C_δ atoms of the side chain (Figure S6A in SI). To confirm the novelty of the binding-induced H-pocket, we also identified the corresponding residues of potential H-pockets in other PDEs by sequence alignment (Figure S7 in SI). Then, we systematically examined all published PDE−inhibitor complex structures in the PDB but could not find any ligand that binds to such a subpocket.

Another interesting finding from our structures is that the binding of **1** to the active site also employs the so-called glutamine-switch mechanism[18] with the conserved residue Gln859 as the purine-binding site. Human PDEs were classified into three groups according to their substrate specificities: cAMP-specific, cGMP-specific, and dual-specific. According to the glutamine-switch mechanism, to recognize both cAMP and cGMP, the side chain of the conserved glutamine in the dual-specific PDEs (Q859 in PDE2A) could rotate freely to form hydrogen bonds with either the exocyclic amino group of cAMP or the exocyclic carbonyl oxygen of cGMP (Figure 3); in the monospecific PDEs, the conserved glutamine recognizes only the cAMP or cGMP due to its interactions with

dx.doi.org/10.1021/ja404449g | J. Am. Chem. Soc. 2013, 135, 11708−11711

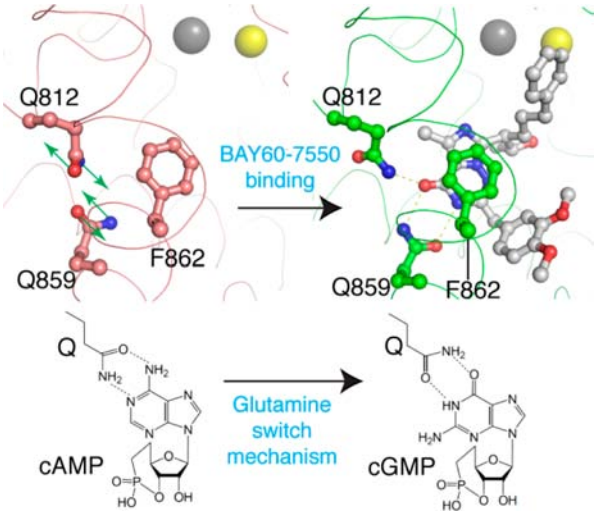

Figure 3. Glutamine-switch mechanism of PDE2A.

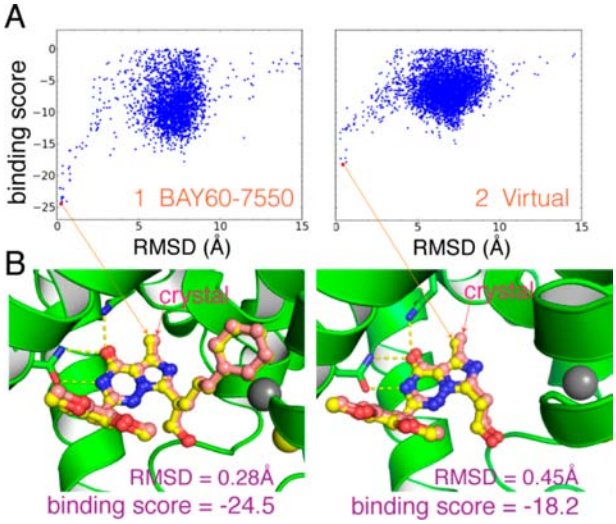

Figure 4. Molecular docking. (A) Computed energy landscapes of **1** and **2**, where those poses with a binding score greater than zero are not shown. (B) Superposition of the lowest-energy docking poses with the crystal structure.

surrounding residues. However, there were also some observations not consistent with this view, e.g., in the dual-specific PDE10 the invariant glutamine is locked by nearby residues.[19] In our apo structure, we found that the side chain of Q859 presents the conformation specific for cAMP binding (Figure 3). However, as seen in Figures 1A and 3, **1** actually is a cGMP analogue. Thus, it is not surprising that in the complex structure, upon the binding of **1**, Q859 rotates its side chain to change to the cGMP-specific conformation and thereby forms two hydrogen bonds with the purine ring of **1**. Moreover, this interaction is further enhanced by another hydrogen bond between the exocyclic carbonyl oxygen of **1** and Gln812, the side chain of which also undergoes rotational change (Figure 3). Sequence alignment shows that equivalent residues of Gln812 in other PDEs are essentially nonpolar, most frequently a proline (indicated by green arrow in Figure S7 in SI). It seems that the glutamine-switch mechanism with an additional glutamine is unique for PDE2A.

On the basis of our findings above, it is reasonable to speculate that both the binding of the propylphenyl group to the H-pocket and the glutamine-switch mechanism may contribute to the inhibitor selectivity. To further clarify this, we employed the Rosetta docking approach that performs large-scale docking with full ligand and receptor flexibility[20] to investigate the binding affinities of **1** with all PDEs for which the crystal structures were available in the PDB (Table S2 in SI). To validate this approach, we first performed docking for PDE2A on the basis of the solved complex structure. The docking energy landscape, obtained by 5000 docking decoys, is shown in Figure 4A, with the crystal structure of **1** as the RMSD reference. As shown, the RMSD of the lowest-score pose with respect to the crystal structure is significantly small and equal to 0.28 Å (Figure 4B), indicating that the docking was in excellent agreement with the crystal structure. Particularly, the funnel-shaped energy landscape shows that the lowest-score pose is located deeply in the funnel bottom, strongly suggesting that this binding pose possesses the highest binding affinity. In addition, validating dockings using our apo structure and two other PDE2 complex structures in the PDB also agreed well with experiments (Figure S8 in SI).

The validating dockings inspired us to use the same approach to examine a virtual molecule derived from **1** (**2** in Figure 1A). As shown, this virtual molecule resembles **1** but lacks the propylphenyl group and could be used to investigate the effects of this group on the inhibitor binding. Results for docking **2** into PDE2A from 5000 Rosetta docking trajectories are shown in Figure 4. As seen, the energy landscape of **2** is very similar to that of **1**, except for the funnel depth. The lowest-score pose of **2** is also in very good agreement with the corresponding part of **1** in the crystal structure, with an RMSD of 0.45 Å (Figure 4B). The high similarity between **1** and **2** indicates that the propylphenyl group does not affect the overall topology of **1** in the active site. It is likely that the glutamine-switch mechanism is the major determinant for the overall binding topology of **1** in the active site, by forming specific hydrogen bonds with the purine ring. Therefore, we conclude that the glutamine-switch mechanism plays an important role in coordinating the overall topology of the inhibitor in the active site.

Although the overall binding topologies of **1** and **2** are almost the same, the differences in the energy funnel depths clearly indicate that the propylphenyl group of **1** does have contributions to the binding affinity by decreasing the binding score (energy) from −18.2 to −24.5 (in Rosetta energy units) (Figure 4B). To estimate this energy decrease in the units of kcal·mol^{-1}, we used the AutoDock empirical energy function[21] to calculate the binding free energies on the basis of the lowest-score poses and found that this decrease in free energy is about −3.2 kcal·mol^{-1}. Thus, the energy contribution from the propylphenyl group may provide for **1** about 220-fold higher binding affinity than that for **2**. Because the propylphenyl group is completely buried in the H-pocket, such contributions can be attributed to the van der Waals interactions between this group and the H-pocket residues. No doubt additional binding affinity could also be a major determinant of the inhibitor selectivity for the given PDEs. Therefore, it is reasonable to deduce that the van der Waals interactions between the propylphenyl group of **1** and the H-pocket of PDE2A are the structural origins of the high inhibitor selectivity. For the other PDEs, equivalent interactions by that group might not be strong enough, and therefore, the affinities of **1** with other PDEs are relatively low. To test this hypothesis, we employed the docking approach to perform an *in silico* affinity profiling for **1** across all the PDEs

dx.doi.org/10.1021/ja404449g | J. Am. Chem. Soc. 2013, 135, 11708−11711

for which the structures were available in the PDB during the period of this study (Table S2 in SI).

The profiling results showed that the overall topology of the lowest-energy pose of **1** in the active site is almost the same in all the PDEs: the purine ring binds to the Q-pocket by the glutamine-switch mechanism; also, in most PDEs the potential H-pockets were induced by the inhibitor binding (Figure S9 in SI). However, as indicated by the Rosetta binding scores in Figure S9 in SI, the calculated binding affinities for other PDEs are less than that of **1** with PDE2A (i.e., −24.5). Similar to those in Figure S8 in SI, the relative values in the binding score implied that the interactions of **1** with the PDE2A H-pocket are the most favorable and thus explain the high selectivity of **1** for PDE2A. As listed in Table S3 in SI, in various PDEs the enclosing residues of the potential H-pocket are essentially hydrophobic, indicating again that the interactions with the H-pocket in nature are hydrophobic. However, due to the varied side-chain sizes of the H-pocket residues, the pocket spaces that could be induced by the inhibitor might be different in various PDEs. Likely, the interplay between the hydrophobic group of the inhibitor and the H-pocket residues is a major determinant of the selectivity for a specific PDE isoform.

In summary, the crystal structures in this study revealed that the highly selective, nanomolar inhibitor **1** binds to the PDE2 active site by using not only the conserved glutamine-switch mechanism for the substrate binding but also a binding-induced, hydrophobic pocket that was not reported previously. Further *in silico* affinity profiling also indicated that binding to the H-pocket has made significant contributions to the binding affinity and thereby improves the inhibitor selectivity for PDE2. Therefore, inhibitors that are able to bind to the potential H-pocket of a given PDE isoform could possess high selectivity for that PDE. Thus, our results provide new structural insights into the PDE inhibitor selectivity and suggest that it is possible to exploit the potential binding-induced pockets to develop isoform-selective PDE inhibitors.

■ ASSOCIATED CONTENT

Supporting Information

Full details on protein expression and purification, crystallography, and molecular docking. Also present are the coordinates of the lowest-energy docking models of PDE-inhibitor complexes investigated in the study. This material is available free of charge via the Internet at http://pubs.acs.org. Data for the apo PDE2A and the PDE2A/BAY60-7550 complex structures have been deposited in the Protein Data Bank with accession codes 4HTZ and 4HTX, respectively.

■ AUTHOR INFORMATION

Corresponding Author

huangqiang@fudan.edu.cn

Notes

The authors declare no competing financial interest.

■ ACKNOWLEDGMENTS

This work was supported in part by the grants from the Hi-tech Research and Development Program of China (No. 2008AA02Z311), the Shanghai Leading Academic Discipline Project (B111), the Shanghai Natural Science Foundation (No. 13ZR1402400), and Shanghai Medicilon Inc. The X-ray diffraction data were collected at the Shanghai Synchrotron Radiation Facility (SSRF), and we thank Dr. Feng Yu for assistance with the collection. We also thank Peter H. Rehse, Ming He, and Jun Wang from Shanghai Medicilon Inc. for helpful discussions and insights.

■ REFERENCES

(1) Bender, A. T.; Beavo, J. A. *Pharmacol. Rev.* **2006**, *58*, 488.
(2) Keravis, T.; Lugnier, C. *Br. J. Pharmacol.* **2012**, *165*, 1288.
(3) Packer, M.; Carver, J. R.; Rodeheffer, R. J.; Ivanhoe, R. J.; DiBianco, R.; Zeldis, S. M.; Hendrix, G. H.; Bommer, W. J.; Elkayam, U.; Kukin, M. L.; Mallis, G. I.; Sollano, J. A.; Shannon, J.; Tandon, P. K.; DeMets, D. L. *New Engl. J. Med.* **1991**, *325*, 1468.
(4) Fabbri, L. M.; Beghe, B.; Yasothan, U.; Kirkpatrick, P. *Nat. Rev. Drug Discovery* **2010**, *9*, 761.
(5) Rotella, D. P. *Nat. Rev. Drug Discovery* **2002**, *1*, 674.
(6) Menniti, F. S.; Faraci, W. S.; Schmidt, C. J. *Nat. Rev. Drug Discovery* **2006**, *5*, 660.
(7) Boess, F. G.; Hendrix, M.; van der Staay, F. J.; Erb, C.; Schreiber, R.; van Staveren, W.; de Vente, J.; Prickaerts, J.; Blokland, A.; Koenig, G. *Neuropharmacology* **2004**, *47*, 1081.
(8) Rutten, K.; Prickaerts, J.; Hendrix, M.; van der Staay, F. J.; Sik, A.; Blokland, A. *Eur. J. Pharmacol.* **2007**, *558*, 107.
(9) Sierksma, A. S.; Rutten, K.; Sydlik, S.; Rostamian, S.; Steinbusch, H. W.; van den Hove, D. L.; Prickaerts, J. *Neuropharmacology* **2013**, *64*, 124.
(10) Domek-Lopacinska, K.; Strosznajder, J. B. *Brain Res.* **2008**, *1216*, 68.
(11) van Donkelaar, E. L.; Rutten, K.; Blokland, A.; Akkerman, S.; Steinbusch, H. W.; Prickaerts, J. *Eur. J. Pharmacol.* **2008**, *600*, 98.
(12) Masood, A.; Nadeem, A.; Mustafa, S. J.; O'Donnell, J. M. *J. Pharmacol. Exp. Ther.* **2008**, *326*, 369.
(13) Ke, H.; Wang, H. *Curr. Top. Med. Chem.* **2007**, *7*, 391.
(14) Pandit, J.; Forman, M. D.; Fennell, K. F.; Dillman, K. S.; Menniti, F. S. *Proc. Natl. Acad. Sci. U.S.A.* **2009**, *106*, 18225.
(15) Plummer, M. S.; Cornicelli, J.; Roark, H.; Skalitzky, D. J.; Stankovic, C. J.; Bove, S.; Pandit, J.; Goodman, A.; Hicks, J.; Shahripour, A.; Beidler, D.; Lu, X. K.; Sanchez, B.; Whitehead, C.; Sarver, R.; Braden, T.; Gowan, R.; Shen, X. Q.; Welch, K.; Ogden, A.; Sadagopan, N.; Baum, H.; Miller, H.; Banotai, C.; Spessard, C.; Lightle, S. *Bioorg. Med. Chem. Lett.* **2013**, *23*, 3438.
(16) LaVallie, E. R.; Lu, Z.; Diblasio-Smith, E. A.; Collins-Racie, L. A.; McCoy, J. M. *Methods Enzymol.* **2000**, *326*, 322.
(17) Card, G. L.; England, B. P.; Suzuki, Y.; Fong, D.; Powell, B.; Lee, B.; Luu, C.; Tabrizizad, M.; Gillette, S.; Ibrahim, P. N.; Artis, D. R.; Bollag, G.; Milburn, M. V.; Kim, S. H.; Schlessinger, J.; Zhang, K. Y. J. *Structure* **2004**, *12*, 2233.
(18) Zhang, K. Y. J.; Card, G. L.; Suzuki, Y.; Artis, D. R.; Fong, D.; Gillette, S.; Hsieh, D.; Neiman, J.; West, B. L.; Zhang, C.; Milburn, M. V.; Kim, S. H.; Schlessinger, J.; Bollag, G. *Mol. Cell* **2004**, *15*, 279.
(19) Wang, H.; Liu, Y.; Hou, J.; Zheng, M.; Robinson, H.; Ke, H. *Proc. Natl. Acad. Sci. U.S.A.* **2007**, *104*, 5782.
(20) Davis, I. W.; Baker, D. *J. Mol. Biol.* **2009**, *385*, 381.
(21) Morris, G. M.; Huey, R.; Lindstrom, W.; Sanner, M. F.; Belew, R. K.; Goodsell, D. S.; Olson, A. J. *J. Comput. Chem.* **2009**, *30*, 2785.